Original Article

Construction of a disulfidptosis-associated lncRNA signature to predict prognosis in bladder cancer

Jingsong Wang[1,2#], Qingyuan Zheng[1,2#], Jun Jian[1,2], Zhiyuan Chen[1,2], Xiuheng Liu[1,2], Shanshan Wan[3], Lei Wang[1,2]

[1]Department of Urology, Renmin Hospital of Wuhan University, Wuhan, China; [2]Institute of Urologic Disease, Renmin Hospital of Wuhan University, Wuhan, China; [3]Department of Ophthalmology, Renmin Hospital of Wuhan University, Wuhan, China

Contributions: (I) Conception and design: J Wang, Q Zheng, J Jian; (II) Administrative support: Z Chen, X Liu, S Wan, L Wang; (III) Provision of study materials or patients: J Wang, Q Zheng; (IV) Collection and assembly of data: J Wang, Q Zheng; (V) Data analysis and interpretation: J Wang, Q Zheng, J Jian; (VI) Manuscript writing: All authors; (VII) Final approval of manuscript: All authors.

[#]These authors contributed equally to this work.

Correspondence to: Shanshan Wan, MD. Department of Ophthalmology, Renmin Hospital of Wuhan University, No. 238 Zhang Zhidong Road, Yellow Crane Tower Street, Wuhan 430060, China. Email: ophwss@whu.edu.cn; Lei Wang, MD. Department of Urology, Renmin Hospital of Wuhan University, No. 238 Zhang Zhidong Road, Yellow Crane Tower Street, Wuhan 430060, China; Institute of Urologic Disease, Renmin Hospital of Wuhan University, Wuhan, China. Email: drwanglei@whu.edu.cn.

Background: Bladder cancer (BCa) is the most common neoplasm of the urinary system, and its high rates of progression and recurrence contribute to a generally poor prognosis, especially in advanced cases. It is reported that disulfidptosis is closely related with tumor proliferation. We aimed to construct a disulfidptosis-associated long non-coding RNA (lncRNA) signature that can predict prognosis and immune microenvironment in BCa.

Methods: We obtained RNA-seq data, clinical information, and mutation data of BCa patients from The Cancer Genome Atlas (TCGA) database. Based on Pearson correlation and uni-Cox regression analysis, we identified disulfidptosis-associated lncRNAs related with overall survival (OS). Then a prognosis signature based on seven disulfidptosis-associated lncRNAs was constructed by least absolute shrinkage and selection operator (LASSO) Cox regression analysis and multi-Cox regression analysis. We performed Gene Ontology (GO), Kyoto Encyclopedia of Genes and Genomes (KEGG), and Gene Set Enrichment Analysis (GSEA) analyses to examine biological functional of differentially expressed genes related to the risk model. We assessed the immune microenvironment and chemotherapeutic response of several drugs. Finally, the quantitative real-time reverse transcription polymerase chain reaction (qRT-PCR) was used to detect the expression level of the disulfidptosis-associated lncRNAs.

Results: We established a prognosis signature based on seven disulfidptosis-associated lncRNAs (AP003419.3, AL161891.1, AC234917.3, LINC00536, AL021707.6, AL445649.1 and AC104785.1). According to the signature, all patients were divided in high- and low-risk group and patients in low-risk group showed a significantly better prognosis. Moreover, the risk model was confirmed to be an independent prognostic factor with high accuracy. Immune cells and several immune checkpoints were more active in high-risk group and patients in this group had a higher tumor mutation burden (TMB) that those in low-risk group. The results of qRT-PCR demonstrated that expression level of the lncRNAs were all significantly different between BCa cell lines and normal urinary epithelial cells.

Conclusions: The disulfidptosis-associated lncRNA signature is a promising biomarker for predicting prognosis and characterizing the immune landscape in BCa, potentially guiding personalized treatment strategies.

Keywords: Disulfidptosis; long non-coding RNA (lncRNA); signature; prognosis; bladder cancer (BCa)

Submitted Aug 20, 2024. Accepted for publication Dec 04, 2024. Published online Dec 27, 2024.
doi: 10.21037/tau-24-431
View this article at: https://dx.doi.org/10.21037/tau-24-431

Introduction

Bladder cancer (BCa) ranks as the tenth most prevalent cancer globally and stands out as the most common urological neoplasms (1). Due to its elevated rates of progression and recurrence, BCa has constituted a formidable threat to human health and carried a substantial economic burden (2). Presently, the precise pathogenesis of BCa remains unclear. Smoking is widely acknowledged as a primary contributor to BCa and exposure to carcinogens represents a common risk factor. In addition, a notable gender disparity exists in BCa incidence, with a higher occurrence among male patients compared to female patients (3,4). According to the depth of muscle invasion, BCa can be categorized into non-muscle invasive bladder cancer (NMIBC), comprising approximately 70% of newly diagnosed BCa, and muscle invasive bladder cancer (MIBC). Based on current treatment guidelines, the standard approach for NMIBC involves surgical resection followed by intravesical therapy (5). Despite prompt treatment, a proportion around 60–80% of NMIBC cases experience eventually recurrence (6). In recent years, chemotherapy and immunotherapy have demonstrated promising outcomes in preventing and treating recurrence and progression of BCa. However, challenges such as resistance, adverse reactions, and other drawbacks persist as significant obstacles (7). Therefore, there is an urgent need for the identification of effective prognostic biomarkers and the exploration of new therapeutic targets for BCa.

Disulfidptosis, a new form of metabolism-related cell death was initially documented by Liu and its partners (8). This phenomenon arises from the intracellular buildup of disulfides in glucose-deprived cells featuring elevated expression of solute carrier family 7 member 11 (SLC7A11). Its characteristic is that the intracellular accumulation of disulfides leads to the collapse of cytoskeletal proteins and F-actin and has been proved to play an important role in tumor growth regulation (9). Nevertheless, the specific mechanisms through which it influences tumor proliferation remains elusive.

Long non-coding RNA (lncRNA) is defined as a transcript with over 200 nucleotides and no protein-coding potential (10). Despite not encoding proteins, LncRNAs are intricately involved in various aspects of cell biology. Recent evidence highlights their role in tumor growth, proliferation, and invasion (11-13). Researches on their role in BCa are also burgeoning. For instance, LncRNA HOTMAIR has been proven to influence BCa progression and the EGFR-ProT-NF-κB-HOTAIR signaling axis takes a part in cisplatin-induced cachexia in BCa (14). Another study has reported that lncRNA AGAP2-AS1 can promote BCa progression and metastasis by recruiting IGF2BP2 to enhance the stability of LRG1 (15). Liu and her team have confirmed that lncRNA UCA1 regulates IMPDH1/2-mediated guanine nucleotide production via TWIST1, which is crucial for BCa cell proliferation, migration, and invasion (16). These findings underscore the intricate involvement of lncRNAs in the molecular mechanisms underlying BCa progression.

Our study investigated the role of disulfidptosis-associated lncRNAs in BCa prognosis. We developed a risk model that accurately predicted BCa outcomes and assessed the immune microenvironment. The model also

Highlight box

Key findings

- We identified a seven-long non-coding RNA (lncRNA) signature associated with disulfidptosis that could predict prognosis in bladder cancer (BCa) patients. High-risk patients in this model exhibited worse prognosis, higher tumor mutation burden, and more active immune cell infiltration, suggesting the potential for immunotherapy applications.

What is known and what is new?

- BCa is highly recurrent with limited treatment options, and several molecular markers have been studied as potential prognostic indicators.
- This study introduced a new disulfidptosis-associated lncRNA signature, revealing its role in prognosis prediction and its correlation with immune cell activity, suggesting its potential in immunotherapy.

What is the implication, and what should change now?

- The disulfidptosis-associated lncRNA signature could serve as a valuable prognostic tool and a target for future therapeutic strategies in BCa.
- Validation in larger cohorts and exploration of its use in clinical immunotherapy trials are necessary to establish its clinical utility.

forecasted responses to chemotherapy and immunotherapy, which provided new diagnostic markers and therapeutic targets for BCa. We present this article in accordance with the TRIPOD and MDAR reporting checklists (available at https://tau.amegroups.com/article/view/10.21037/tau-24-431/rc).

Methods

Data acquisition

The RNA-seq data, clinical data and gene mutation annotation data of BCa patients were downloaded from The Cancer Genome Atlas (TCGA) database (https://tcga-data.nci.nih.gov/tcga/). To ensure the integrity of the dataset, BCa cases lacking complete information on survival time and clinical features were systematically excluded and the remaining dataset was subsequently utilized for subsequent in-depth analyses. The study was conducted in accordance with the Declaration of Helsinki (as revised in 2013).

Identification of disulfidptosis-associated lncRNAs

Pearson correlation and co-expression analyses were executed to pinpoint disulfidptosis-associated lncRNAs. Specifically, lncRNAs exhibiting a correlation coefficient greater than 0.4 and a P value less than 0.001 were considered for further analysis. The connection between disulfidptosis-associated genes and disulfidptosis-associated lncRNAs was established using the "Limma" R package, incorporating criteria of |logFC| greater than 1 and a corrected P value below 0.05.

Construction and validation of prognosis risk model based on disulfidptosis-associated lncRNAs

In our study, all BCa patients were randomly assigned to training and test cohorts using the "caret" R package to ensure robust model validation. We initiated our analysis with univariate Cox (uni-COX) regression to identify disulfidptosis-associated lncRNAs that were significantly associated with overall survival (OS), defined by a P value of ≤0.05. Following this, we employed the least absolute shrinkage and selection operator (LASSO) regression, which included 10-fold cross-validation and maintained a P value threshold of ≤0.05. This step was crucial for selecting the most relevant OS-related lncRNAs while minimizing overfitting. We then constructed a prognostic risk model based on multivariate Cox (multi-Cox) proportional hazards regression, utilizing the selected lncRNAs. The risk scores for each patient were calculated using the following formula:

$$\text{Risk score} = \sum_{i=1}^{n} \text{coefficient of lncRNA}_i \times \text{expression of lncRNA}_i \quad [1]$$

After calculating the risk scores, we categorized BCa patients into high- and low-risk groups based on their median risk scores. Kaplan-Meier analysis was subsequently performed to evaluate the OS of these two risk groups. To assess the predictive accuracy of our risk model, we calculated the area under the receiver operating characteristic curve (AUROC) and the concordance index (C-index). Additionally, we conducted both uni- and multi-Cox regression analyses to verify that the model's predictions were independent of various clinical features.

Function enrichment analysis

First, we utilized principal component analysis (PCA) to classify the expression patterns of disulfidptosis-associated lncRNAs and the spatial dispersion of two risk group patients was visualized based on the "limma" and "scatteredplot3" R packages. To gain insights into the biological functions and pathways associated with differentially expressed disulfidptosis-associated genes, we performed Gene Ontology (GO), Kyoto Encyclopedia of Genes and Genomes (KEGG), and Gene Set Enrichment Analysis (GSEA) analyses. These analyses were conducted using the "clusterProfiler" and "enrichplot" R packages, with significance defined as P<0.05 and false discovery rate (FDR) <0.25.

Assessment of the immune microenvironment

We calculated the StromalScore, ImmuneScore, and ESTIMATEScore (calculated as the sum of StromalScore and ImmuneScore) of each BCa patients utilizing the "limma" and "estimate" R packages. To further evaluate the immunological profiles, we assessed the percentage of immunocyte infiltration and assigned scores to the immunocyte infiltration using the "limma", "parallel", "reshape2" and "ggpubr" R packages. Then the Single-Sample GSEA (ssGSEA) and the "GSVA" R package were used to delve into the differences in immune function between the two risk groups. Finally, we conducted a comparative analysis of the expression levels of several immune checkpoints in the high- and low-risk groups.

Tumor mutation burden (TMB) and drug sensitivity analysis

We determined the TMB of BCa patients in the high- and low-risk groups utilizing somatic mutation data, and this analysis was performed with the assistance of the "maftools" R package. In addition, we assessed the half-maximal inhibitory concentration (IC_{50}) of various chemotherapy drugs to gain insights into the drug sensitivity of BCa patients in the different risk groups using the "oncoPredict" R packages.

Cluster analysis

Using the "ConsensusClusterPlus" R package, we performed a classification of patients into three subtypes based on the expression levels of disulfidptosis-associated lncRNAs in relation to the risk model. Then we conducted analyses on survival status and response to immunotherapy within the identified subtypes using various R packages, including "survival", "Rtsne", "limma", and "reshape2".

Cell culture

The cell lines were procured from American-Type Culture Collection (ATCC). The two BCa cell lines (T24, 5637) were cultured in RPMI 1640 (HyClone, China) supplemented with 10% fetal bovine serum media while the human immortalized uroepithelial (SV-HUC-1) cell line was cultured in Ham's F-12K (HyClone, China) supplemented with 10% fetal bovine serum (Gibco, Australia) media. Standard cell culture conditions were maintained, with all cell lines being passaged in an incubator containing 5% CO_2 at 37 ℃.

Quantitative real-time reverse transcription polymerase chain reaction (qRT-PCR)

Initially, total RNA from the three cell lines (T24, 5637, and SV-HUC-1) was extracted using TRIzol reagent (Thermo Fisher Scientific, Massachusetts, USA). Following RNA extraction, reverse transcription was carried out using the reverse transcription kit from Servicebio to synthesize complementary DNA (cDNA). Subsequently, qRT-PCR was conducted on the Quanta gene q225 real-time PCR system. The experimental setup involved the use of specific primers for the targeted genes, and all primer sequences employed are detailed in Table S1.

Statistics analysis

All data were analyzed by R software (version 4.2.2) and GraphPad Prism 8.0. The Wilcox rank-sum test was used to compare the differences between two groups. Statistical significance was determined as $P<0.05$ for all two-tailed tests.

Results

Identification of disulfidptosis-associated lncRNAs and establishment of the risk signature

Firstly, we retrieved RNA-seq data of BLCA patients from the TCGA-BLCA database, encompassing 19 normal and 406 tumor samples. Then protein coding mRNAs and lncRNAs were discriminated and we identified disulfidptosis-associated lncRNAs through Pearson correlation analysis, examining the co-expression patterns of disulfidptosis genes with lncRNAs ($|\text{Pearson R}| >0.4$ and $P<0.001$). The relationship between disulfidptosis genes and these associated lncRNAs is visually represented in *Figure 1A*. Next, we obtained 22 disulfidptosis-associated lncRNAs significantly correlated with OS in BCa patients by uni-Cox regression analysis (*Figure 1B*). The heatmap illustrated the correlation between the seven model lncRNAs and disulfidptosis genes (*Figure 1C*). Further refinement of the prognostic model involved employing LASSO Cox regression and multi-Cox regression analyses, culminating in the selection of seven key lncRNAs to formulate the prognostic model (*Figure 1D*,*1E*). Based on the expression level and regression coefficient of each lncRNAs, we calculated the risk score of each BCa patient according to the following formula:

$$\begin{aligned}\text{Risk score} = {} & \text{AP003419.3}\times(-0.2685831)+\text{AL161891.1}\times(0.3440701)\\ & +\text{AC234917.3}\times(0.4402398)+\text{LINC00536}\times(0.2625216)\\ & +\text{AL021707.6}\times(-0.2464479)+\text{AL445649.1}\times(0.3631754)\\ & +\text{AC104785.1}\times(-0.4109131)\end{aligned} \quad [2]$$

Evaluation and validation of the prognostic risk model

All the patients were categorized into high- and low-risk group according to the median risk scores. In *Figure 2*, we presented the risk scores, survival status of patients, and expression levels of the seven selected lncRNAs for the entire cohort, as well as the separate train and test cohorts. As anticipated, patients in the high-risk group exhibited a poorer prognosis (year) across all three cohorts, underscoring the robust prognostic significance of the

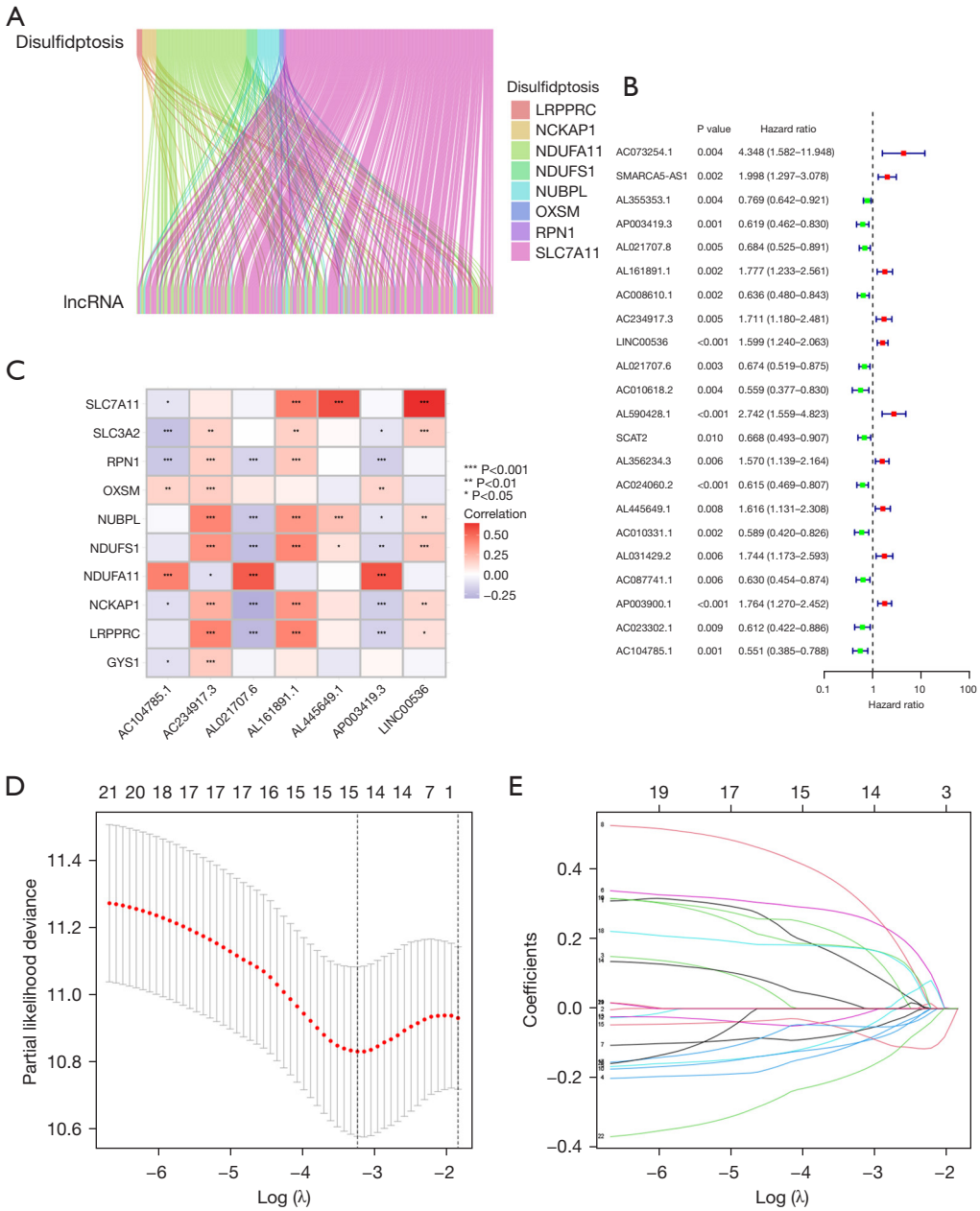

Figure 1 Construction of the disulfidptosis-related lncRNAs risk signature. (A) Sankey diagram of lncRNAs related with disulfidptosis genes. (B) The forest plot of prognostic disulfidptosis-related lncRNAs obtained by uni-Cox analysis. (C) Correlations between disulfidptosis-related lncRNAs of the risk signature and disulfidptosis genes. (D) LASSO coefficients of disulfidptosis-related lncRNAs. (E) Cross-validation of disulfidptosis-related lncRNAs in the LASSO regression. lncRNA, long non-coding RNA; LASSO, least absolute shrinkage and selection operator.

risk model. To assess whether the risk model served as an independent prognostic factor beyond other clinical characteristics, we performed univariate and multivariate Cox regression analyses. The results revealed that the risk score, along with age (year) and tumor stage, emerged as independent prognostic indicators in BCa patients (*Figure 3A,3B*). ROC curve analysis was applied to further validate the predictive accuracy of the risk model. The area

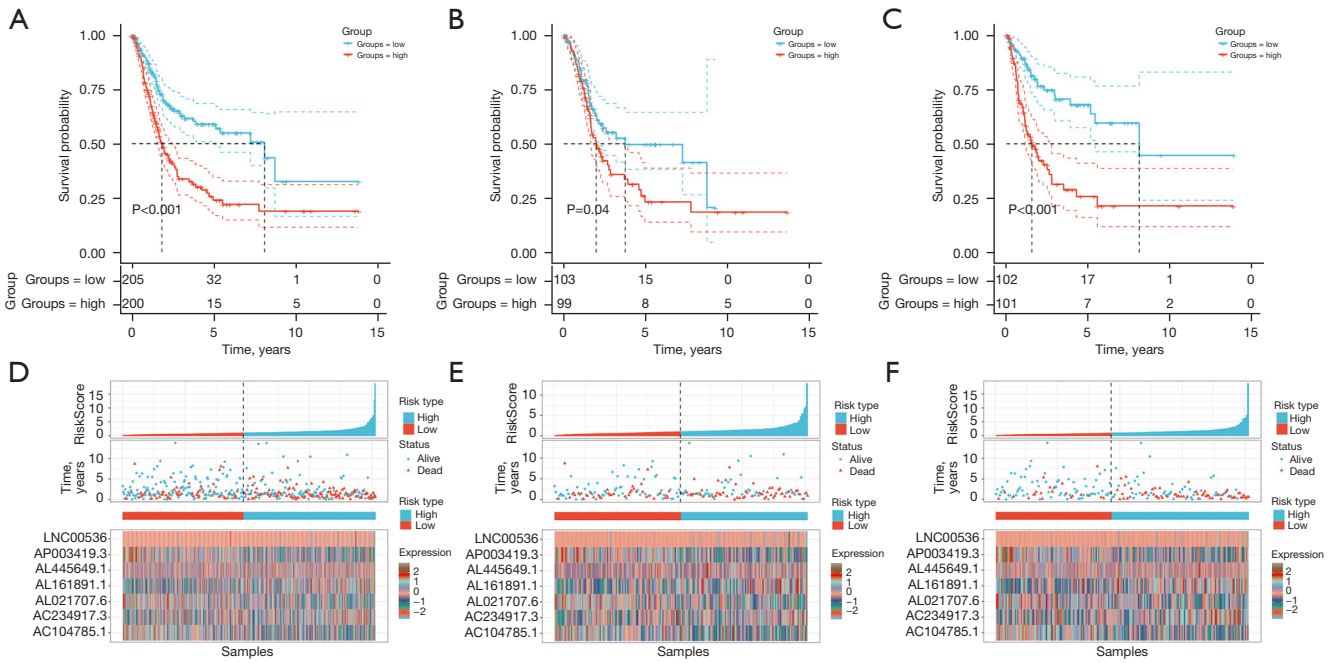

Figure 2 Prognosis evaluation of the risk signature. (A-C) Kaplan-Meier survival analysis of BCa patients in the entire, train, and test cohorts, respectively; (D-F) Expression levels of seven lncRNAs, survival time and survival status of BCa patients in the entire, train, and test cohorts, respectively. BCa, bladder cancer; lncRNA, long non-coding RNA.

under curves (AUCs) of the 1-, 3-, and 5-year survival rates were 0.640, 0.685 and 0.703 (*Figure 3C*). Notably, the AUC of the risk score was 0.685, significantly outperforming other clinical characteristics such as age (0.617), gender (0.491), grade (0.465), and stage (0.642) (*Figure 3D*). This indicated that the risk model exhibited superior predictive capability compared to traditional clinical features. In addition, the C-index curves further supported these findings, illustrating the enhanced discriminatory power of the risk model (*Figure 3E*). Furthermore, based on the risk model, we investigated the survival probabilities in high- and low-risk groups stratified by clinical features (*Figure 4*). The results showed that patients in high-risk groups consistently exhibited notably poorer OS compared to those in the low-risk groups, irrespective of age (≥65 or <65 years), gender (male or female) and clinical stages (stage I–II or stage III/IV), reinforcing the ability of the risk model to predict BCa prognosis independently of various clinical features.

Biological functional analysis of differentially expressed genes

PCA was performed to observe distribution between high- and low-risk groups based on all genes, disulfidptosis-associated genes, disulfidptosis-associated lncRNAs and the risk model. As shown in *Figure 5*, the risk model displayed the best discriminatory ability in distinguishing between high- and low-risk BCa patients. To explore gene enrichments between two risk groups, we performed GO, KEGG and GSEA. The results of GO suggested that disulfidptosis-associated genes were predominantly enriched in various biological process (BP), including signaling receptor activator activity, receptor ligand activity and glycosaminoglycan binding. In regard to molecular function (MF), epidermis development, axon development, external encapsulating structure organization, extracellular structure organization and extracellular matrix (ECM) organization were significantly abundant. Moreover, several cellular components (CC), such as collagen-containing ECM, apical part of cell, apical plasma membrane and basal part of cell were enriched in disulfidptosis-associated genes (*Figure 6A-6C*). Furthermore, the results of KEGG revealed significant pathway enrichments in P13K-Akt signaling pathway, cytokine-cytokine receptor interaction, ECM-receptor interaction and arrhythmogenic right ventricular cardiomyopathy, all of which are important signaling

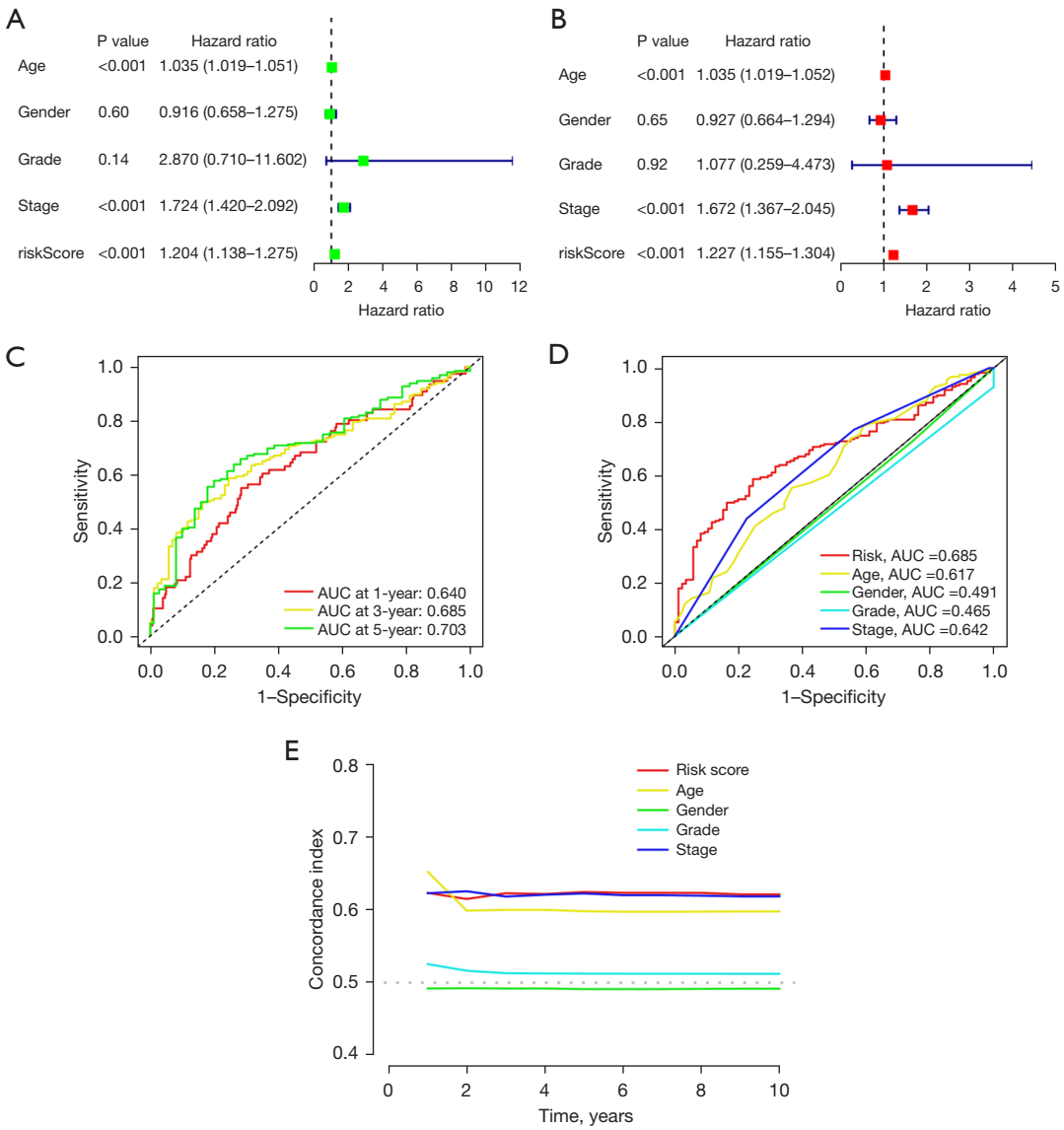

Figure 3 Validation of the risk signature. (A) Uni-Cox regression analysis of clinical features and risk score. (B) Multi-Cox regression analysis of clinical features and risk score. (C) The ROC curves of 1-, 3-, and 5-year survival rates. (D) The ROC curves of the risk model and clinical features; (E) C-index curves of the risk model and clinical features. AUC, area under curve; ROC, receiver operating characteristic.

pathways related to tumorigenesis and tumor progression (*Figure 6D,6E*). In addition, according to GSEA, we found that disulfidptosis-associated genes were primarily enriched in sensory perception of smell, RNA interference (rnai) effector complex, odorant binding, olfactory receptor activity and translation repressor activity in low-risk group. In contrast, cell-cell adhesion via plasma membrane adhesion molecule, homophilic cell adhesion via plasma membrane adhesion molecule, intermediate filament, intermediate filament cytoskeleton and keratin filament were abundant in high-risk group (*Figure 6F,6G*).

Tumor immune microenvironment based on prognosis risk model

We examined the immune microenvironment in BCa

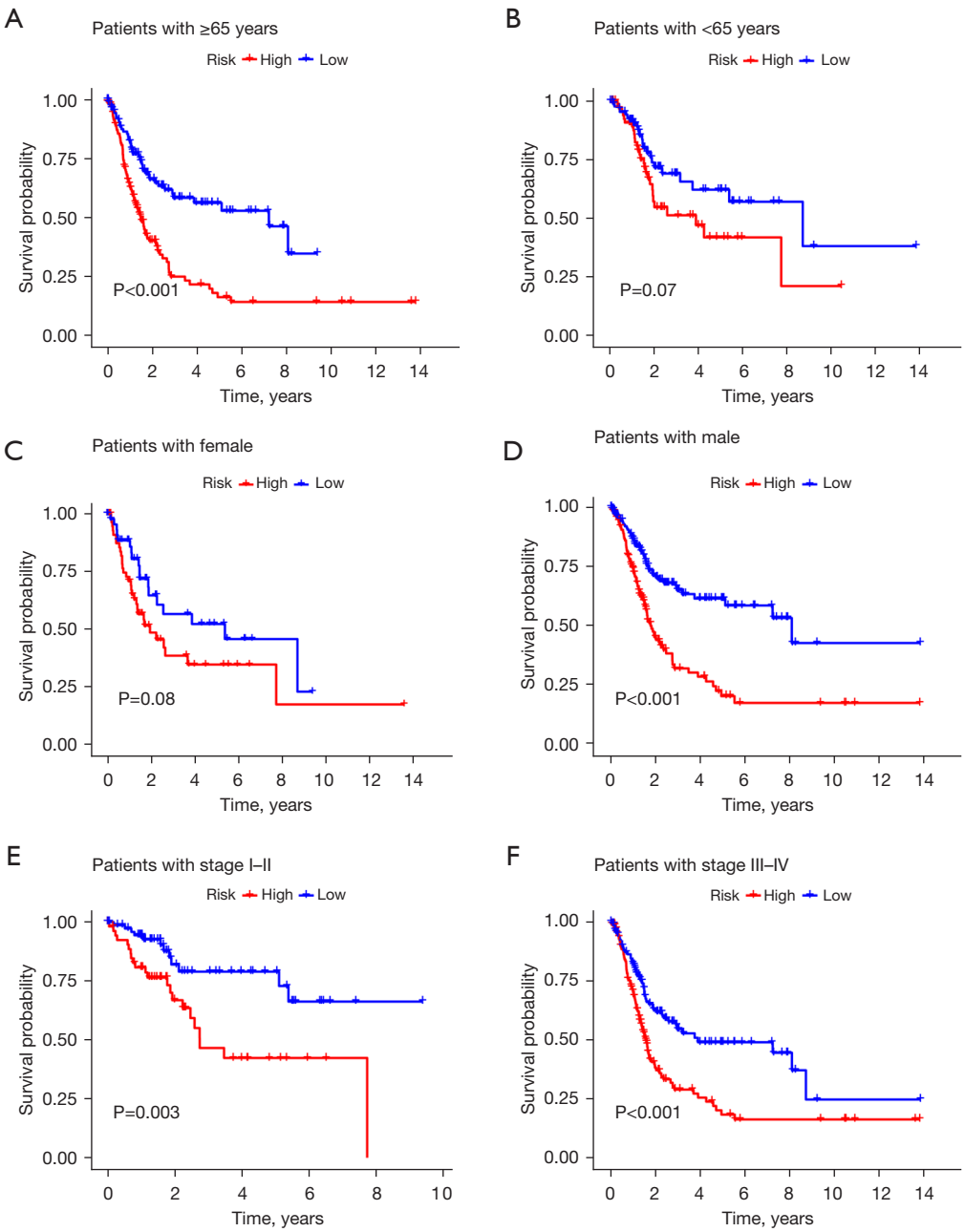

Figure 4 The Kaplan-Meier survival analysis of patients with different clinical features. (A,B) Age (≥65 and <65 years). (C,D) Gender (female and male). (E,F) Stage (stage I–II and stage III–IV).

patients based on the risk model. The results of the TIME analysis showed that patients in high-risk group exhibited higher stromalscore, immunescore, and ESTIMATEscore than those in low-risk group, which indicated that stromal cells and immune cells were more active in high-risk patients, leading to a higher likelihood tumor progression and metastasis (*Figure 7A*). Next, we investigated the relationship between risk scores and tumor immunocyte infiltration. In *Figure 7B*, we could find that the fractions of resting T cells CD4 memory and macrophages M0 were higher in high-risk group while the fractions of plasma cells and regulatory T cells were higher in low-

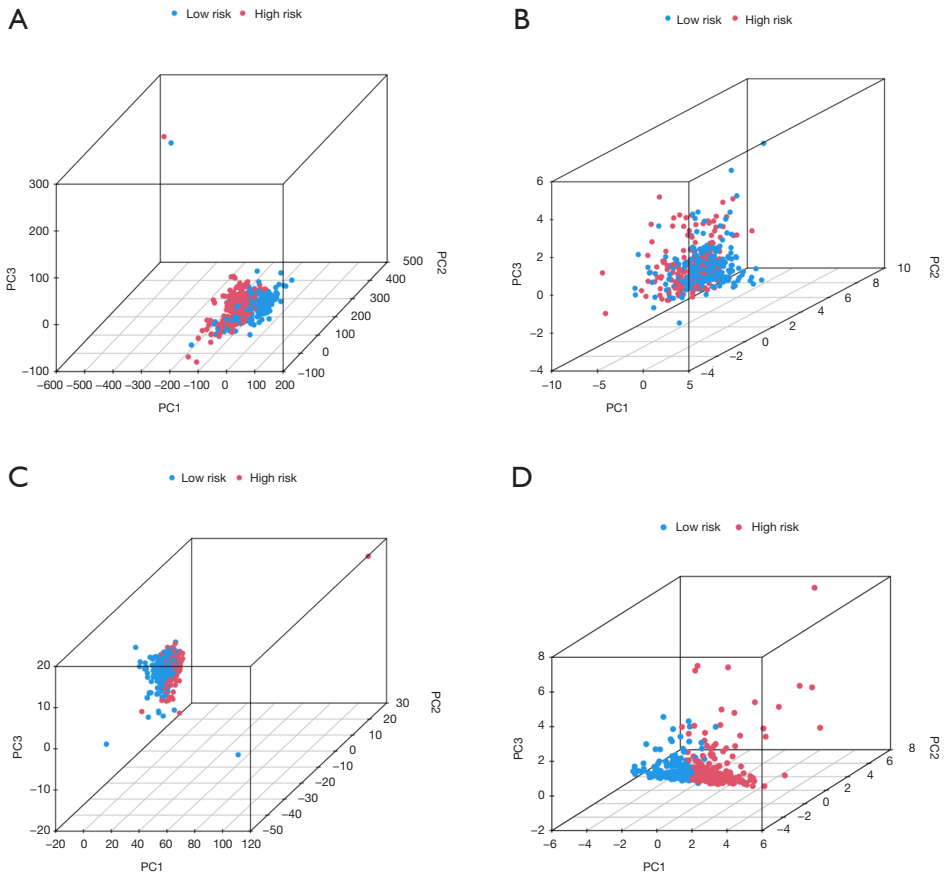

Figure 5 Principal component analysis. (A) PCA of total genes. (B) PCA of disulfidptosis genes. (C) PCA of disulfidptosis-related lncRNAs; (D) PCA of the seven disulfidptosis-related lncRNAs used in the risk signature. PCA, principal component analysis; lncRNA, long non-coding RNA.

risk group. What's more, we analyzed immune functions between the two risk groups. *Figure 7C* showed that most immune cells, including activated dendritic cells (aDCs), B cells, $CD8^+$ T cells, mast cells, macrophages, neutrophils, plasmacytoid dendritic cells (pDCs), T helper cells, T follicular helper cells, Th1 cells, tumor-infiltrating lymphocyte, and T regulatory cells, had high scores in high-risk group. And various immune functions, such as antigen presenting cell (APC) co-inhibition, APC co-stimulation, chemokine receptor (CCR), checkpoint, cytolytic activity, human leukocyte antigen, inflammation-promoting, parainflammation, T cell co-inhibition, T cell co-stimulation and type I interferon (IFN) response were significantly enriched in high-risk group. Above outcomes implied that immune functions were more active in high-risk group and high-risk patients might be more sensitive to immunotherapy. Besides, several immune checkpoints were quantified. We found that some immune checkpoints, including CD28, TNFRSF9, ICOS, CD274, IDO1, TNFRSF8, NRP1 and so on showed a higher expression in high-risk group, suggesting that patients in this group might be more responsive to potential immunotherapy (*Figure 7D*). *Figure 7E* illustrated the relative proportions of various immune cell types in the high- and low-risk groups, with the results corroborating the above discussed findings.

TMB characteristic based on prognosis risk model

We analyzed and compared tumor-related gene mutation frequency and TMB between the two risk groups. As shown in *Figure 8A,8B*, 188 (94.95%) of 198 samples in the high-risk group exhibited a higher TMB compared to the low-risk group (90.59%). And the examination uncovered the 15 most frequently mutated genes, including *TP53*, *TTN*,

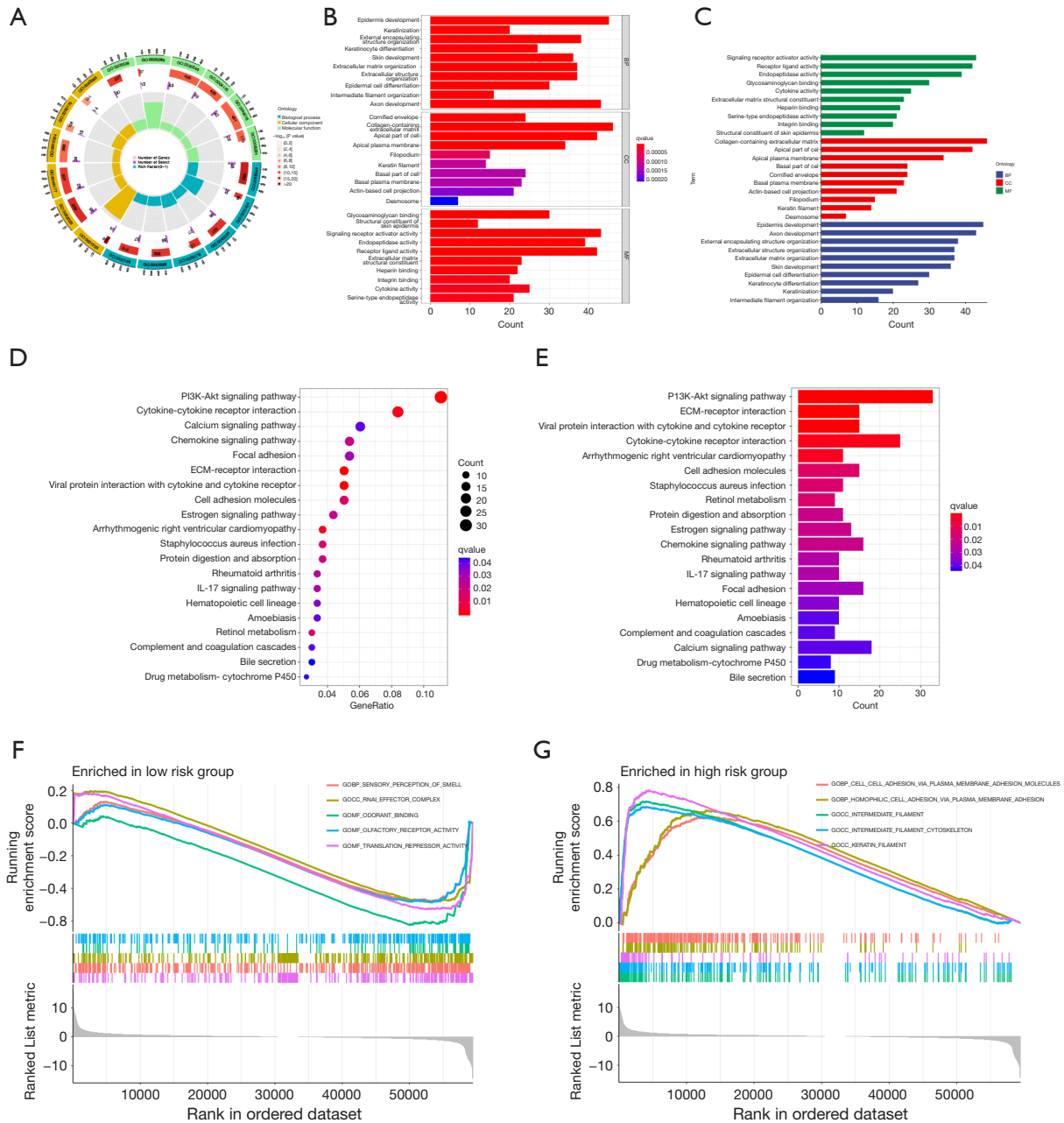

Figure 6 Biological functional and pathway enrichment analysis. (A-C) GO functional enrichment analysis; (D,E) KEGG pathways enrichment analysis; (F,G) GESA pathways enrichment analysis in low- and high-risk groups. BP, biological process; CC, cellular component; MF, molecular function; ECM, extracellular matrix; IL, interleukin; GO, Gene Ontology; KEGG, Kyoto Encyclopedia of Genes and Genomes; GESA, Gene Set Enrichment Analysis.

KMT2D, *MUC16*, *ARID1A*, *KDM6A*, *PIK3CA*, *SYNE1*, *RYR2*, *KMT2C*, *HMCN1*, *RB1*, *FAT4*, *MACF1* and *FLG*, most of which had mutation frequencies in high-risk group. According to the survival curves, we found that high TMB patients had a better prognosis than low TMB patients (*Figure 8C*). Then we combined the effects of risk score and TMB on the OS of BCa patients. The results indicated that patients with the lowest risk score and highest TMB had

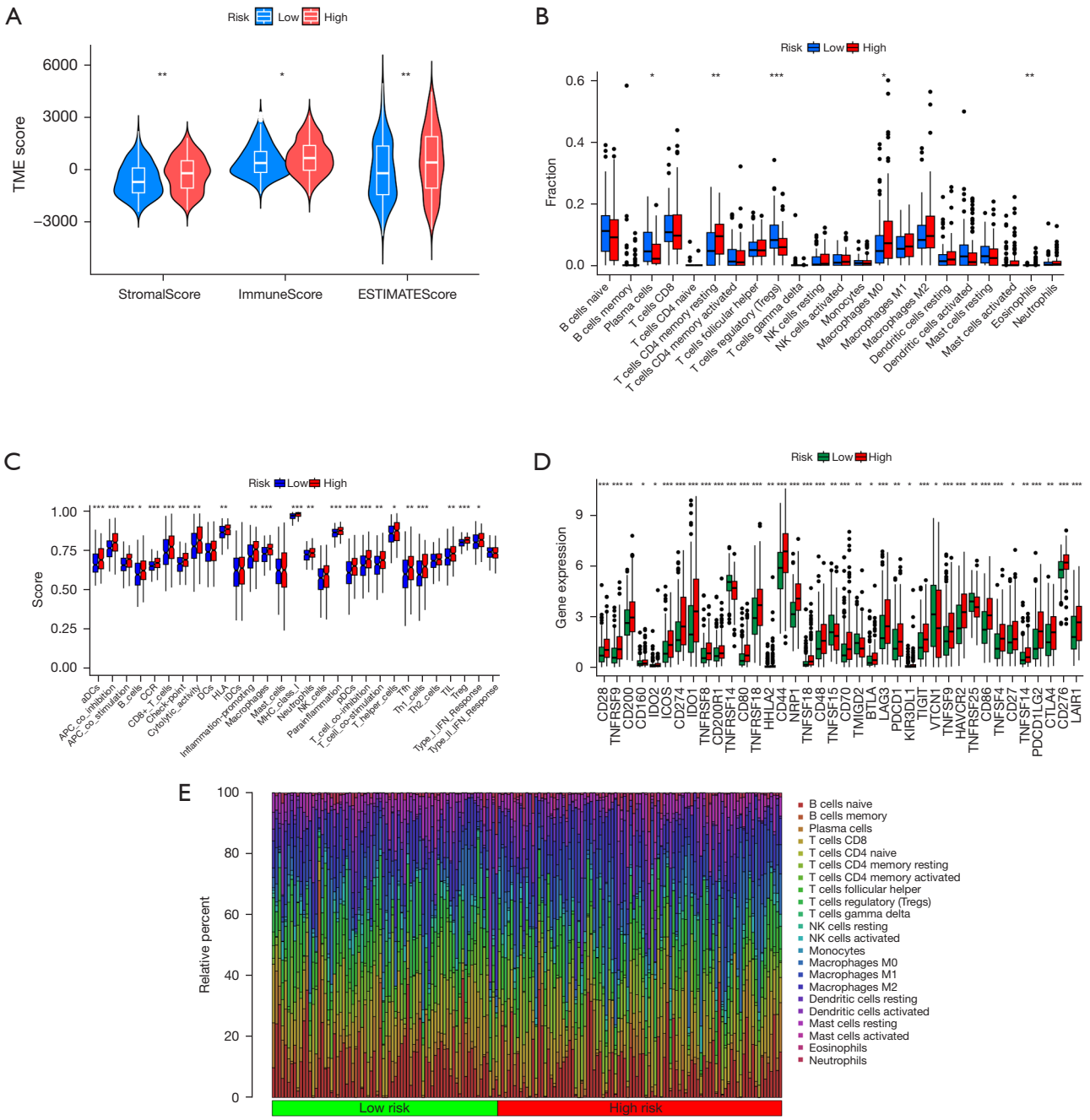

Figure 7 Tumor immune microenvironment analysis. (A) Violin plot of the stromal (P=0.002), immune (P=0.04), and ESTIMATE (P=0.007) scores in high- and low-risk groups (ESTIMATE scores = stromal scores + immune scores). (B) Immunocyte infiltration percentages in two risk groups. (C) ssGESA scores of 16 immune cells and 13 immune functions. (D) The expression levels of common immune checkpoints in the risk groups. (E) Barplot of immunocyte infiltration relative percentages. *, P<0.05; **, P<0.01; ***, P<0.001. TME, tumor microenvironment; ESTIMATE, Estimation of Stromal and Immune cells in malignant tumor tissues using Expression data; NK, natural killer; ssGESA, single-sample Gene Set Enrichment Analysis.

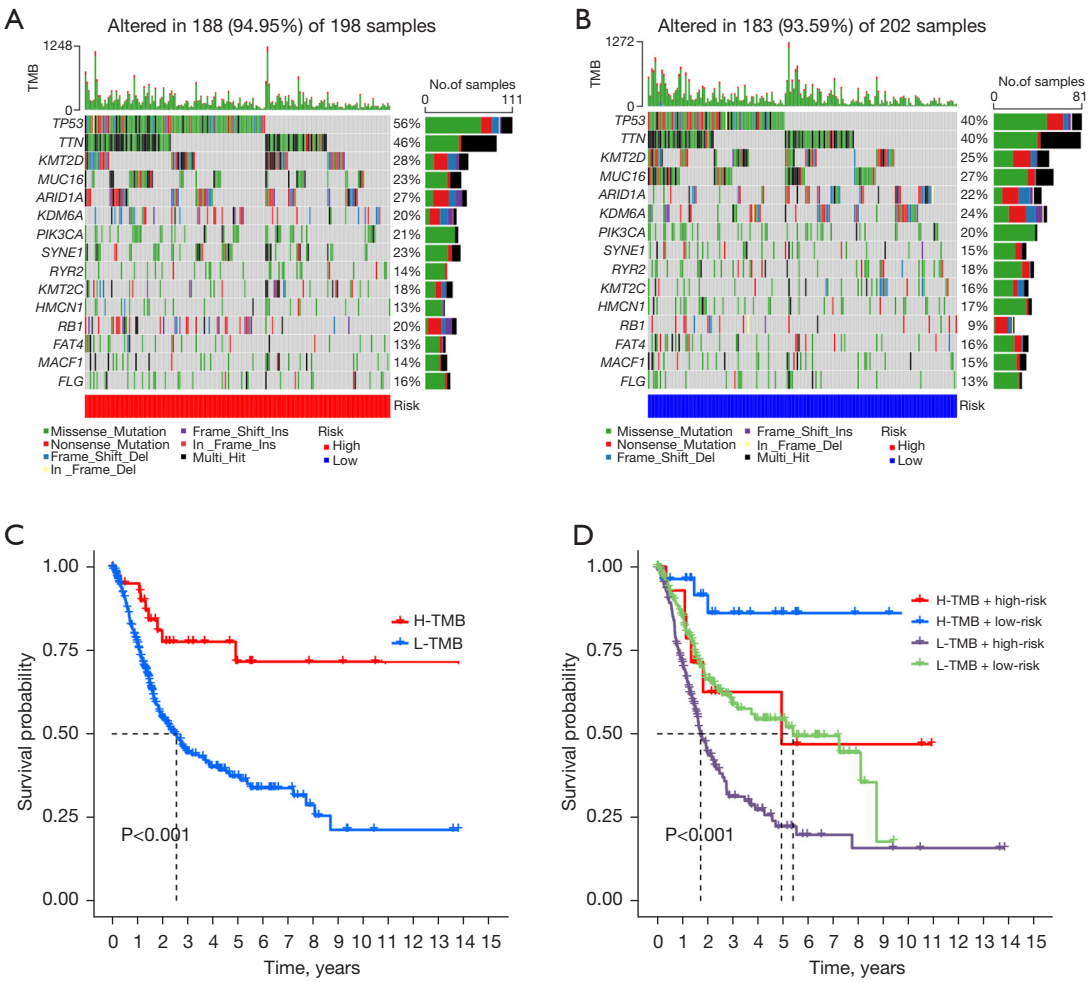

Figure 8 TMB characteristic. (A,B) Tumor somatic mutation waterfall plot in high- and low-risk groups. (C) Kaplan-Meier survival analysis for TMB; (D) Kaplan-Meier survival analysis for TMB and risk groups. TMB, tumor mutation burden; H, high; L, low.

the best prognosis whereas those with highest risk score and lowest TMB had the worst prognosis (*Figure 8D*).

Drug sensitivity in BCa based on prognosis risk model

We investigated the associations between risk score and sensitivity to chemotherapy drugs using IC_{50} values as a measure of sensitivity. Compared with low-risk group, Sorafenib, Nilotinib and AZD2014 exhibited higher IC_{50} values in high-risk group, indicating that these drugs might be more suitable for patients in low-risk group. Conversely, cisplatin, olaparib and talazoparib showed higher IC_{50} values in low-risk patients, which suggested that patients in low-risk would more sensitive to these drugs (*Figure 9*).

Cluster analysis based on prognosis risk model

To explore the immune microenvironment in different tumor subtypes, we performed a cluster analysis based on the risk model. We classified all BCa patients into three clusters through the "ConsensusClusterPlus" package (*Figure 10A*). *Figure 10B* exhibited that the majority of high-risk patients were sorted into cluster 1 and 3 while those patients in cluster 2 belonged to low-risk group. The survival analysis revealed that patients in cluster 2 represented the most favorable prognosis, followed by cluster 1 and patients in cluster 3 had the least favorable prognosis (*Figure 10C*). PCA and t-Distributed Stochastic Neighbor Embedding (t-SNE) were used to verify the distinction between these

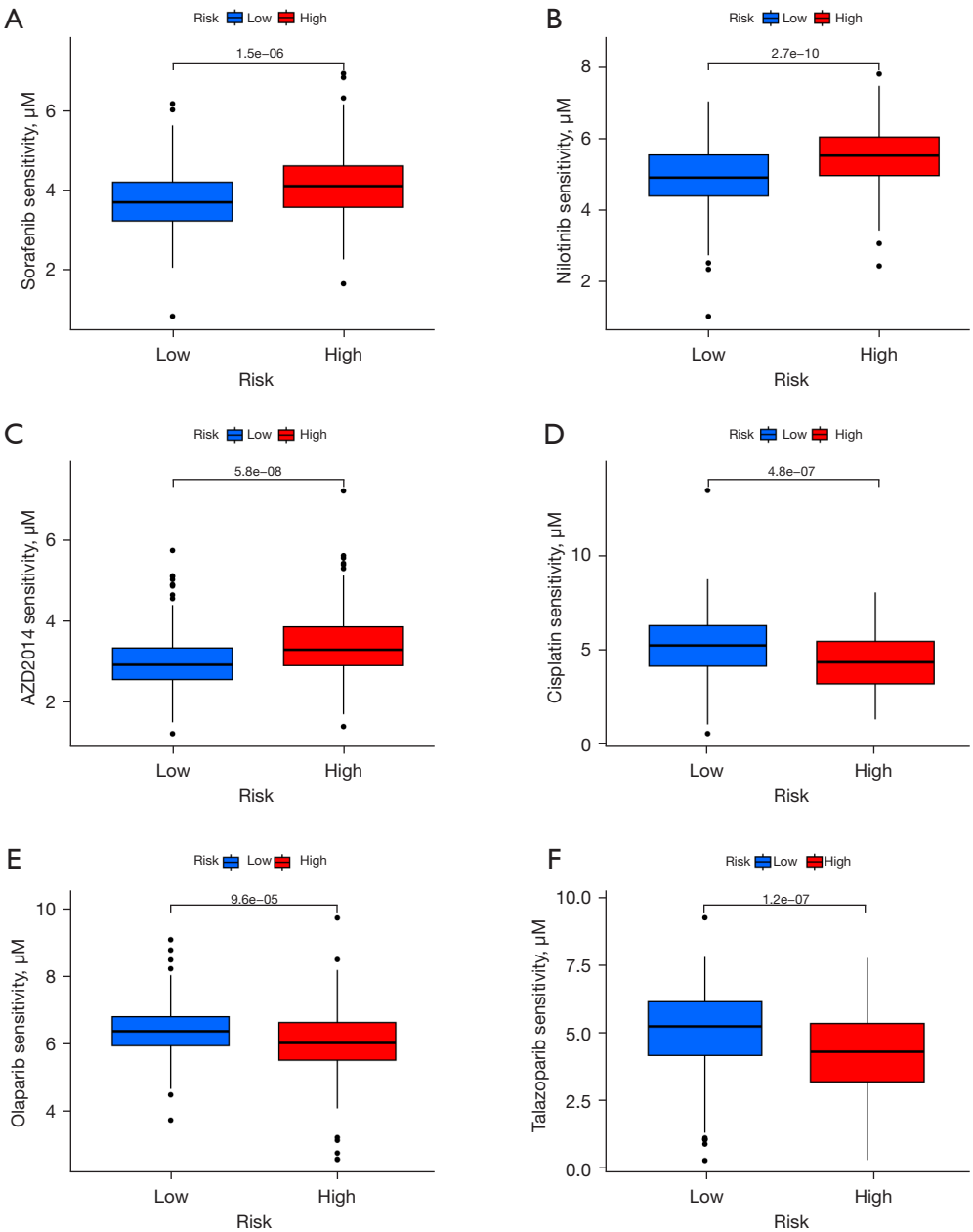

Figure 9 Drug sensitive prediction. (A-F) IC_{50} values (μM) of several chemotherapy drugs in BCa. (A) Sorafenib. (B) Nilotinib. (C) AZD2014. (D) Cisplatin. (E) Olaparib. (F) Talazoparib. IC_{50}, half maximal inhibitory concentration; BCa, bladder cancer.

three clusters (*Figure 10D-10G*). Furthermore, we assessed the activity of various immune checkpoints in each cluster, with the majority showing significantly higher activity in clusters 1 and 3 (*Figure 10H*). In addition, cluster 1 demonstrated lower immunescore, stromalscore, and ESTIMATEscore compared to clusters 2 and 3, aligning with the previous findings (*Figure 10I-10K*).

Expression of the lncRNAs in the risk model

The qRT-PCR was performed to detect the expression level of the lncRNAs included in the risk model. As displayed in *Figure 11*, AL161891.1, LINC00536 and AL445649.1 exhibited higher expression in two BCa cell lines compared to normal urinary epithelial cells while AP003419.3,

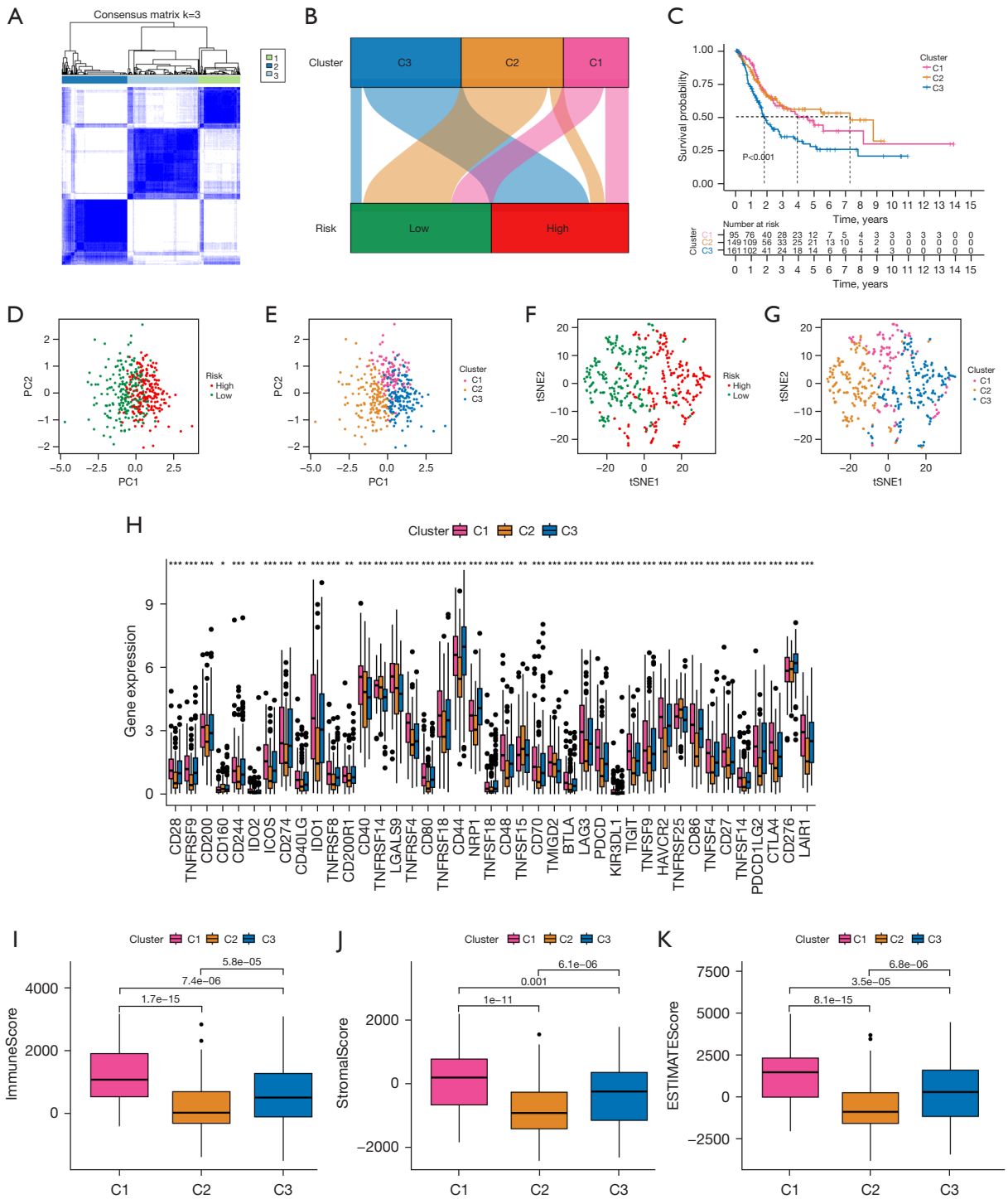

Figure 10 Cluster analysis of the risk model. (A) All patients were divided into three clusters according to the consensus clustering matrix (k=3). (B) Sankey diagram of the three clusters and two risk groups. (C) Kaplan-Meier survival analysis for the three clusters. (D,E) PCA of the two risk groups and three clusters. (F,G) t-SNE of the two risk groups and three clusters. (H) The expression levels of immune checkpoints in the three clusters. (I-K) Violin plot of the immune, stromal, and ESTIMATE scores in three clusters. *, P<0.05; **, P<0.01; ***, P<0.001. t-SNE, t-Distributed Stochastic Neighbor Embedding; ESTIMATE, Estimation of Stromal and Immune cells in malignant tumor tissues using Expression data; PCA, principal component analysis.

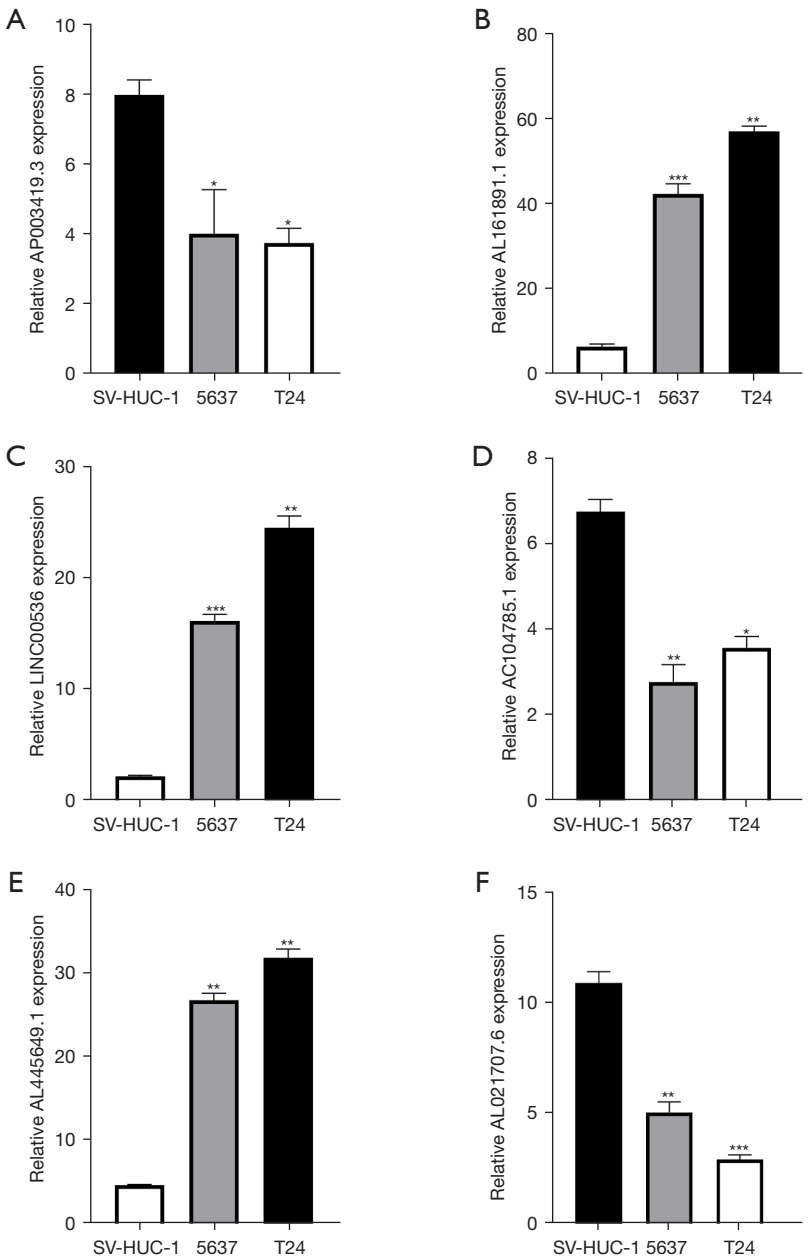

Figure 11 Expression of disulfidptosis-related lncRNAs in BCa cell lines. (A-F) Relative expression levels of AP003419.3 (P=0.04; P=0.03), AL161891.1 (P<0.001; P=0.006), LINC00536 (P<0.001; P=0.004), AC104785.1 (P=0.005; P=0.03), AL445649.1 (P=0.006; P=0.003) and AL021707.6 (P=0.007; P<0.001) in two BCa cell lines (5637, T24) and SV-HUC-1 cell line. *, P<0.05; **, P<0.01; ***, P<0.001. lncRNAs, long non-coding RNAs; BCa, bladder cancer.

AC104785.1 and AL021707.6 showed opposite results.

Discussion

BCa is the most common tumor of urinary system, ranking as the sixth most common tumor in men and the 17th in women (17). With over 90% originating from urothelial cells, BCa is characterized by inherent invasiveness, leading to a high recurrence rate (18). Surgical resection remains the primary treatment, necessitating postoperative

chemotherapy and immunotherapy to deter relapse. Despite these efforts, the limited efficacy of chemotherapy and immunotherapy, influenced by various factors, results in a 5-year relapse-free survival rate of less than 43% (19,20). Therefore, it is imperative to delve into the mechanisms of BCa development, enhance early diagnosis and treatment strategies, and thereby mitigating recurrence and metastasis.

Disulfidptosis, distinct from cuproptosis and ferroptosis, is a recently identified mode of cell death (8). In glucose-starved tumor cells with high expression of SLC7A11, the accumulation of disulfide bond substances disrupts the normal binding of disulfide bonds between cytoskeletal proteins, leading to histone skeleton collapse and cell death. Subsequent studies have also confirmed its association with tumor progression (21-23). Recently, there have been studies to predict the prognosis of BCa by constructing cuproptosis or ferroptosis-related lncRNA model (24,25). Chen *et al.* established a disulfidptosis-related gene prognostic model to enhance the survival and drug sensitivity of BCa patients (26). However, whether disulfidptosis-related lncRNAs can serve as a prognostic marker for BCa has not been explored yet. In this study, our primary objective was to explore the impact of disulfidptosis-associated lncRNAs on the prognosis of BCa. We systematically identified lncRNAs associated with disulfidptosis to develop a comprehensive risk model. This model demonstrated a high degree of accuracy in predicting the prognosis of BCa and allowed for an in-depth analysis of the immune microenvironment, immunotherapy and chemotherapy reactivity, providing a new perspective for improving the survival of BCa patients.

First, we identified 22 disulfidptosis-related lncRNAs associated with prognosis, with seven lncRNAs (AP003419.3, AL161891.1, AC234917.3, LINC00536, AL021707.6, AL445649.1, AC104785.1) chosen to construct the model based on LASSO, uni- and multi-Cox regression analyses. Many fundamental researches have demonstrated the effects of LNC00536 in various tumors such as hepatocellular carcinoma (27), breast cancer (28) and BCa (29). We randomly divided the TCGA-BLCA cohort into train and test subsets, with patients categorized into high- and low-risk groups based on LASSO-calculated risk scores. High-risk patients exhibited poorer prognosis, and the risk model outperformed traditional tumor node and metastasis (TNM) staging and other clinical-pathological staging in predicting BCa prognosis. The results of KEGG suggested that P13K-Akt signaling pathway and ECM-receptor interaction were enriched in disulfidptosis-related genes. According to previous studies (30-32), P13K-Akt signaling pathway was closely bound up with the occurrence and progression of many tumors. In BCa, corilagin inhibited BC cell migration, invasion, and metastasis through the repression of the NF-κB mediated P13K/Akt signaling pathway (33). In the same way, ECM-receptor interaction was an important segment in tumor development (34). Lots of studies have also pointed out its emphasis in BCa (35,36).

The tumor immune environment is a complex environment, encompassing not only immune cells, but also immune checkpoints, regulatory cells and inflammatory cytokines, which is the primary factors of tumor invasion and migration, as well as the determining factor of immunotherapy response (37). Our study revealed heightened stromal and immune cell enrichment in the high-risk group, correlating with poorer prognosis. High-risk patients demonstrated more active immune functions, suggesting potential efficacy in immunotherapy. Furthermore, the expression levels of various immune checkpoints, including CD28, TNFRSF9, ICOS, CD274, IDO1, TNFRSF8, NRP1, have significantly increased in high-risk group. We could infer that these patients might exhibit heightened immune reactivity and benefit more from immune checkpoint inhibitor (ICI) treatment. Of course, further research is essential to determine if inhibitors targeting these checkpoints hold promise as anti-tumor drugs for BCa.

TMB is defined as the total number of mutations present in the tumor specimen. A higher TMB indicates increased production of new antigens, potentially triggering T cell responses. As a result, TMB is generally considered a biomarker for immunotherapy (38,39). TMB has a good predictive value in response to immunotherapy for BCa (40). In this study, compared to low-risk group, patients in high-risk group exhibited a higher TMB, further confirming the notion that these patients would benefit more from immunotherapy.

Certainly, there are several shortcomings in our study. First, our data only came from a single database (TCGA). Because we were unable to obtain comprehensive lncRNA annotations and clinical information from databases such as Gene Expression Omnibus (GEO) and International Cancer Genome Consortium (ICGC). The selections for lncRNAs were limited. Second, although we performed PCR to verify the difference expression of the lncRNAs in two kinds of BCa cell lines, validation in clinical BCa samples was unexecuted. Finally, our study was simply based on bioinformatics analysis, further experiments are necessary to establish the specific mechanisms of the lncRNAs in BCa.

Conclusions

We established a disulfidptosis-associated lncRNA signature that can predict prognosis and reflect the immune microenvironment in BCa. This seven-lncRNA model serves as an independent prognostic factor, with the low-risk group showing better survival. The high-risk group exhibited increased immune activity and TMB, suggesting potential for immunotherapy. Further validation is needed to confirm its clinical applicability.

Acknowledgments

We thank our colleagues in the Department of Urology, Renmin Hospital of Wuhan University, for their support of this work, as well as all colleagues involved in model development and data collection.

Funding: This research was funded by National Natural Science Foundation of China (No. 82000639).

Footnote

Reporting Checklist: The authors have completed the TRIPOD and MDAR reporting checklists. Available at https://tau.amegroups.com/article/view/10.21037/tau-24-431/rc

Peer Review File: Available at https://tau.amegroups.com/article/view/10.21037/tau-24-431/prf

Conflicts of Interest: All authors have completed the ICMJE uniform disclosure form (available at https://tau.amegroups.com/article/view/10.21037/tau-24-431/coif). The authors have no conflicts of interest to declare.

Ethical Statement: The authors are accountable for all aspects of the work in ensuring that questions related to the accuracy or integrity of any part of the work are appropriately investigated and resolved. The study was conducted in accordance with the Declaration of Helsinki (as revised in 2013).

References

1. Zhang Q, Liu S, Wang H, et al. ETV4 Mediated Tumor-Associated Neutrophil Infiltration Facilitates Lymphangiogenesis and Lymphatic Metastasis of Bladder Cancer. Adv Sci (Weinh) 2023;10:e2205613.
2. Lobo N, Afferi L, Moschini M, et al. Epidemiology, Screening, and Prevention of Bladder Cancer. Eur Urol Oncol 2022;5:628-39.
3. Gilyazova I, Enikeeva K, Rafikova G, et al. Epigenetic and Immunological Features of Bladder Cancer. Int J Mol Sci 2023;24:9854.
4. Maas M, Todenhöfer T, Black PC. Urine biomarkers in bladder cancer - current status and future perspectives. Nat Rev Urol 2023;20:597-614.
5. Martini A, Tholomier C, Mokkapati S, et al. Interferon gene therapy with nadofaragene firadenovec for bladder cancer: from bench to approval. Front Immunol 2023;14:1260498.
6. Lopez-Beltran A, Cookson MS, Guercio BJ, et al. Advances in diagnosis and treatment of bladder cancer. BMJ 2024;384:e076743.
7. Chen H, Yang W, Xue X, et al. Integrated Analysis Revealed an Inflammatory Cancer-Associated Fibroblast-Based Subtypes with Promising Implications in Predicting the Prognosis and Immunotherapeutic Response of Bladder Cancer Patients. Int J Mol Sci 2022;23:15970.
8. Liu X, Nie L, Zhang Y, et al. Actin cytoskeleton vulnerability to disulfide stress mediates disulfidptosis. Nat Cell Biol 2023;25:404-14.
9. Zheng T, Liu Q, Xing F, et al. Disulfidptosis: a new form of programmed cell death. J Exp Clin Cancer Res 2023;42:137.
10. Marima R, Basera A, Miya T, et al. Exosomal long non-coding RNAs in cancer: Interplay, modulation, and therapeutic avenues. Noncoding RNA Res 2024;9:887-900.
11. Ye M, Zhao L, Zhang L, et al. LncRNA NALT1 promotes colorectal cancer progression via targeting PEG10 by sponging microRNA-574-5p. Cell Death Dis 2022;13:960.
12. Azizidoost S, Ghaedrahmati F, Sheykhi-Sabzehpoush M, et al. The role of LncRNA MCM3AP-AS1 in human cancer. Clin Transl Oncol 2023;25:33-47.
13. Shakhpazyan NK, Mikhaleva LM, Bedzhanyan AL,

et al. Long Non-Coding RNAs in Colorectal Cancer: Navigating the Intersections of Immunity, Intercellular Communication, and Therapeutic Potential. Biomedicines 2023;11:2411.
14. Hu CY, Su BH, Lee YC, et al. Interruption of the long non-coding RNA HOTAIR signaling axis ameliorates chemotherapy-induced cachexia in bladder cancer. J Biomed Sci 2022;29:104.
15. Zhao X, Chen J, Zhang C, et al. LncRNA AGAP2-AS1 interacts with IGF2BP2 to promote bladder cancer progression via regulating LRG1 mRNA stability. Cell Signal 2023;111:110839.
16. Liu SS, Li JS, Xue M, et al. LncRNA UCA1 Participates in De Novo Synthesis of Guanine Nucleotides in Bladder Cancer by Recruiting TWIST1 to Increase IMPDH1/2. Int J Biol Sci 2023;19:2599-612.
17. Jubber I, Ong S, Bukavina L, et al. Epidemiology of Bladder Cancer in 2023: A Systematic Review of Risk Factors. Eur Urol 2023;84:176-90.
18. Ho MD, Modi PK. Novel cryotherapy in non-muscle-invasive bladder cancer. Cancer 2023;129:333-4.
19. Meeks JJ, Black PC, Galsky M, et al. Checkpoint Inhibitors in Urothelial Carcinoma-Future Directions and Biomarker Selection. Eur Urol 2023;84:473-83.
20. Tomiyama E, Fujita K, Hashimoto M, et al. Urinary markers for bladder cancer diagnosis: A review of current status and future challenges. Int J Urol 2024;31:208-19.
21. Chen Y, Jin C, Cui J, et al. Single-cell sequencing and bulk RNA data reveal the tumor microenvironment infiltration characteristics of disulfidptosis related genes in breast cancer. J Cancer Res Clin Oncol 2023;149:12145-64.
22. Zhao Y, Wei Y, Fan L, et al. Leveraging a disulfidptosis-related signature to predict the prognosis and immunotherapy effectiveness of cutaneous melanoma based on machine learning. Mol Med 2023;29:145.
23. Liu T, Ren Y, Wang Q, et al. Exploring the role of the disulfidptosis-related gene SLC7A11 in adrenocortical carcinoma: implications for prognosis, immune infiltration, and therapeutic strategies. Cancer Cell Int 2023;23:259.
24. Bai Y, Zhang Q, Liu F, et al. A novel cuproptosis-related lncRNA signature predicts the prognosis and immune landscape in bladder cancer. Front Immunol 2022;13:1027449.
25. Chen M, Nie Z, Li Y, et al. A New Ferroptosis-Related lncRNA Signature Predicts the Prognosis of Bladder Cancer Patients. Front Cell Dev Biol 2021;9:699804.
26. Chen H, Yang W, Li Y, et al. Leveraging a disulfidptosis-based signature to improve the survival and drug sensitivity of bladder cancer patients. Front Immunol 2023;14:1198878.
27. Wang LG, Song HY, Zhang KP, et al. LINC00536 promotes hepatocellular carcinoma progression via the miR-203b-5p/VEGFA axis. Neoplasma 2022;69:136-44.
28. Hu C, Zhang X, Fang K, et al. LINC00536 Promotes Breast Cancer Progression by Regulating ROCK1 via Sponging of miR-214-5p. Biochem Genet 2023;61:1163-84.
29. Li R, Zhang L, Qin Z, et al. High LINC00536 expression promotes tumor progression and poor prognosis in bladder cancer. Exp Cell Res 2019;378:32-40.
30. Zhang J, Pan S, Li Y, et al. Nerolidol inhibits proliferation and triggers ROS-facilitated apoptosis in lung carcinoma cells via the suppression of MAPK/STAT3/NF-κB and P13K/AKT pathways. Adv Clin Exp Med 2024. [Epub ahead of print]. doi: 10.17219/acem/190274.
31. Li Z, Song Y, Hou W, et al. Atractylodin induces oxidative stress-mediated apoptosis and autophagy in human breast cancer MCF-7 cells through inhibition of the P13K/Akt/mTOR pathway. J Biochem Mol Toxicol 2022;36:e23081.
32. Yu T, An Q, Cao XL, et al. GOLPH3 inhibition reverses oxaliplatin resistance of colon cancer cells via suppression of PI3K/AKT/mTOR pathway. Life Sci 2020;260:118294.
33. Yu X, Wu T, Liao B, et al. Anticancer potential of corilagin on T24 and TSGH 8301 bladder cancer cells via the activation of apoptosis by the suppression of NF-κB-induced P13K/Akt signaling pathway. Environ Toxicol 2022;37:1152-9.
34. Dzobo K, Senthebane DA, Dandara C. The Tumor Microenvironment in Tumorigenesis and Therapy Resistance Revisited. Cancers (Basel) 2023;15:376.
35. Wang X, Bai Y, Zhang F, et al. Prognostic value of COL10A1 and its correlation with tumor-infiltrating immune cells in urothelial bladder cancer: A comprehensive study based on bioinformatics and clinical analysis validation. Front Immunol 2023;14:955949.
36. Criscitiello MF, Kraev I, Lange S. Post-Translational Protein Deimination Signatures in Serum and Serum-Extracellular Vesicles of Bos taurus Reveal Immune, Anti-Pathogenic, Anti-Viral, Metabolic and Cancer-Related Pathways for Deimination. Int J Mol Sci 2020;21:2861.
37. Erratum: IGF2BP family of RNA-binding proteins regulate innate and adaptive immune responses in cancer cells and tumor microenvironment. Front Immunol 2023;14:1297519.
38. Chan TA, Yarchoan M, Jaffee E, et al. Development of tumor mutation burden as an immunotherapy biomarker:

utility for the oncology clinic. Ann Oncol 2019;30:44-56.
39. Jardim DL, Goodman A, de Melo Gagliato D, et al. The Challenges of Tumor Mutational Burden as an Immunotherapy Biomarker. Cancer Cell 2021;39:154-73.
40. McGrail DJ, Pilié PG, Rashid NU, et al. High tumor mutation burden fails to predict immune checkpoint blockade response across all cancer types. Ann Oncol 2021;32:661-72.

Cite this article as: Wang J, Zheng Q, Jian J, Chen Z, Liu X, Wan S, Wang L. Construction of a disulfidptosis-associated lncRNA signature to predict prognosis in bladder cancer. Transl Androl Urol 2024;13(12):2705-2723. doi: 10.21037/tau-24-431